1

CHAPTER 1

The role of spatial dispersion of repolarization and intramural reentry in inherited and acquired sudden cardiac death syndromes

Charles Antzelevitch

Abstract

The cellular basis for intramural reentry that develops secondary to the development of transmural dispersion of repolarization (TDR) is examined in this review. The hypothesis that amplification of spatial dispersion of repolarization underlies the development of intramural reentry and life-threatening ventricular arrhythmias associated with inherited ion channelopathies is probed. The roles of TDR in the long-QT, short-QT, and Brugada syndromes as well as catecholaminergic polymorphic ventricular tachycardia are critically examined. In the long-QT syndrome, amplification of TDR is generally secondary to preferential prolongation of the action potential duration (APD) of M cells, whereas in the Brugada syndrome, it is due to selective abbreviation of the APD of right ventricular epicardium. Preferential abbreviation of APD of either endocardium or epicardium appears to be responsible for amplification of TDR in the short-QT syndrome. The available data suggest that the long-QT, short-QT, and Brugada syndromes are pathologies with very different phenotypes and etiologies, but which share a common final pathway in causing sudden cardiac death.

Keywords:

long QT syndrome; short QT syndrome; Brugada syndrome; polymorphic ventricular tachycardia; electrophysiology

Inherited sudden cardiac death secondary to the development of life-threatening ventricular arrhythmias have been associated with a variety of ion channelopathies such as the long-QT, short-QT, and Brugada syndromes. Table 1.1 lists the genetic defects thus far identified to be associated with these primary electrical diseases. These ion channel defects have been shown to amplify spatial dispersion of repolarization, in some cases with the assistance of pharmacologic agents that further exaggerate the gain or loss of function of ion channel activity. Before examining these interactions, we will review the basis for intrinsic electrical heterogeneity within the ventricular myocardium.

Intrinsic electrical heterogeneity within the ventricular myocardium

It is now well established that ventricular myocardium is comprised of at least three electrophysiologically as well as functionally distinct cell types: epicardial, M, and endocardial cells [1,2]. These three principal ventricular myocardial cell types differ with respect to phase 1 and phase 3 repolarization characteristics. Ventricular epicardial and M,

Ventricular Arrhythmias and Sudden Cardiac Death, 1st edition. Edited by P.J. Wang, A. Al-Ahmad, H. Hsia, and P.C. Zei
 ISBN: 978-1-4051-6114-5.

Table 1.1 Inherited disorders caused by ion channelopathies

		Rhythm	*Inheritance*	*Locus*	*Ion channel*	*Gene*
Long-QT syndrome	(RW)	TdP	AD			
	LQT1		AD	11p15	I_{Ks}	*KCNQ1*, *KvLQT1*
	LQT2		AD	7q35	I_{Kr}	*KCNH2*, *HERG*
	LQT3		AD	3p21	I_{Na}	*SCN5A*, $Na_v1.5$
	LQT4		AD	4q25		*ANKB*, *ANK2*
	LQT5		AD	21q22	I_{Ks}	*KCNE1*, *minK*
	LQT6		AD	21q22	I_{Kr}	*KCNE2*, *MiRP1*
	LQT7	(Anderson–Tawil syndrome)	AD	17q23	I_{K1}	*KCNJ2*, *Kir 2.1*
	LQT8	(Timothy syndrome)	AD	6q8A	I_{Ca}	*CACNA1C*, $Ca_v1.2$
	LQT9		AD	3p25	I_{Na}	*CAV3*, *Caveolin-3*
	LQT10		AD	11q23.3	I_{Na}	*SCN4B*, $Na_v b4$
LQT syndrome (JLN)		TdP	AR	11p15	I_{Ks}	*KCNQ1*, *KvLQT1*
				21q22	I_{Ks}	*KCNE1*, *minK*
Brugada syndrome	BrS1	PVT	AD	3p21	I_{Na}	*SCN5A*, *Nav1.5*
	BrS2	PVT	AD	3p24	I_{Na}	*GPD1L*
	BrS3	PVT	AD	12p13.3	I_{Ca}	*CACNA1C*, $Ca_v1.2$
	BrS4	PVT	AD	10p12.33	I_{Ca}	*CACNB2b*, $Ca_v B_{2b}$
Short-QT syndrome	SQT1	VT/VF	AD	7q35	I_{Kr}	*KCNH2*, *HERG*
	SQT2		AD	11p15	I_{Ks}	*KCNQ1*, *KvLQT1*
	SQT3		AD	17q23.1-24.2	I_{K1}	*KCNJ2*, *Kir2.1*
	SQT4		AD	12p13.3	I_{Ca}	*CACNA1C*, $Ca_v1.2$
	SQT5		AD	10p12.33	I_{Ca}	*CACNB2b*, $Ca_v\beta 2b$
Catecholaminergic VT	CVPT1	VT	AD	1q42-43		*RyR2*
	CPVT2	VT	AR	1p13-21		*CASQ2*

Abbreviations: AD, autosomal dominant; AR, autosomal recessive; JLN, Jervell and Lange-Nielsen; LQT, long QT; RW, Romano–Ward; TdP, Torsade de Pointes; VF, ventricular fibrillation; VT, ventricular tachycardia; PVT, polymorphic VT.

but not endocardial, cells generally display a prominent phase 1, due to a large 4-aminopyridine (4-AP)-sensitive transient outward current (I_{to}), giving the action potential either a spike-and-dome or a notched configuration. These regional differences in I_{to} were first suggested on the basis of action potential data [3] and subsequently demonstrated using patch clamp techniques in canine [4], feline [5], rabbit [6], rat [7], ferret [8], and human [9,10] ventricular myocytes.

The magnitude of the action potential notch and corresponding differences in I_{to} have also been shown to be different between right and left ventricular epicardium [11]. Similar interventricular differences in I_{to} have also been described for canine ventricular M cells [12]. This distinction is thought to form the basis for why the Brugada syndrome, a channelopathy-mediated form of sudden death, is a right ventricular disease.

Wang and co-workers [13] reported a larger L-type calcium channel current (I_{Ca}) in canine endocardial versus epicardial ventricular myocytes, although other studies have failed to detect any difference in I_{Ca} among cells isolated from epicardium, M, and endocardial regions of the canine left ventricular wall [14,15]. Myocytes isolated from the epicardial region of the left ventricular wall of the rabbit show a higher density of cAMP-activated chloride current when compared to endocardial myocytes [16]. I_{to2}, initially ascribed to a K^+ current, is now thought to be caused primarily by the calcium-activated chloride current ($I_{Cl(Ca)}$); it is thought to also contribute to the action potential notch but it is not known whether this current

differs among the three ventricular myocardial cell types [17].

Characteristics of the M cell

Residing in the deep structures of the ventricular wall between the epicardial and endocardial layers, are M cells and transitional cells. The M cell, masonic midmyocardial Moe cell, discovered in the early 1990s, was named in memory of Gordon K Moe [2,18,19]. The hallmark of the M cell is that its action potential can prolong more than that of epicardium or endocardium in response to a slowing of rate or in response to agents that prolong APD (Figure 1.1) [1,18,20]. Histologically, M cells are similar to epicardial and endocardial cells. Electrophysiologically and pharmacologically, they appear to be a hybrid between Purkinje and ventricular cells [21]. Like Purkinje fibers, M cells show a prominent APD prolongation and develop early afterdepolarizations (EAD) in response to I_{Kr} blockers, whereas epicardium and endocardium do not. Like Purkinje fibers, M cells develop delayed afterdepolarizations (DAD) more readily in response to agents that calcium load or overload the cardiac cell. α_1 Adrenoceptor stimulation produces APD prolongation in Purkinje fibers, but abbreviation in M cells, and little or no change in endocardium and epicardium [22].

Although transitional cells are found throughout much of the wall in the canine left ventricle, M cells displaying the longest action potentials (at basic cycle lengths (BCLs) $\geq$ 2000 ms) are often localized in the deep subendocardium to midmyocardium in the anterior wall [23], deep subepicardium to midmyocardium in the lateral wall [18], and throughout the wall in the region of the right ventricular (RV) outflow tracts [2]. M cells are also present in the deep cell layers of endocardial structures, including papillary muscles, trabeculae, and the interventricular septum [24]. Unlike Purkinje fibers, M cells are not found in discrete bundles or islets [24,25] although there is evidence that they may be localized in discrete muscle layers. Cells with the characteristics of M cells have been described in the canine, guinea pig, rabbit, pig, and human ventricles [4,18,20,23–44].

Isolated myocytes dissociated from discrete layers of the left ventricular wall display APD values

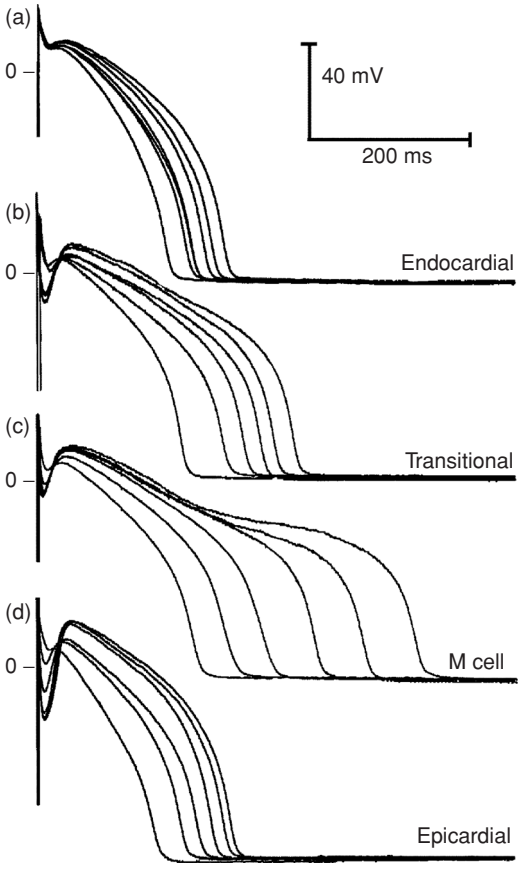

Figure 1.1 Transmembrane activity recorded from cells isolated from the epicardial, M, and endocardial regions of the canine left ventricle at basic cycle lengths (BCL) of 300–5000 milliseconds (steady-state conditions). The M and transitional cells were enzymatically dissociated from the midmyocardial region. Deceleration-induced prolongation of APD is much greater in M cells than in epicardial and endocardial cells. The spike-and-dome morphology is also more accentuated in the epicardial cell. From [4], with permission.

that differ by more than 200 milliseconds at relatively slow rates of stimulation. When the cells are in a functional syncytium that comprises the ventricular myocardium, electrotonic interactions among the different cells types lead to reduction of the APD dispersion to 25–55 milliseconds. The transmural increase in APD from epicardium to endocardium is relatively gradual, except between the epicardium and subepicardium where there is often a sharp increase in APD (Figure 1.2). This has been shown to be due to an increase in tissue

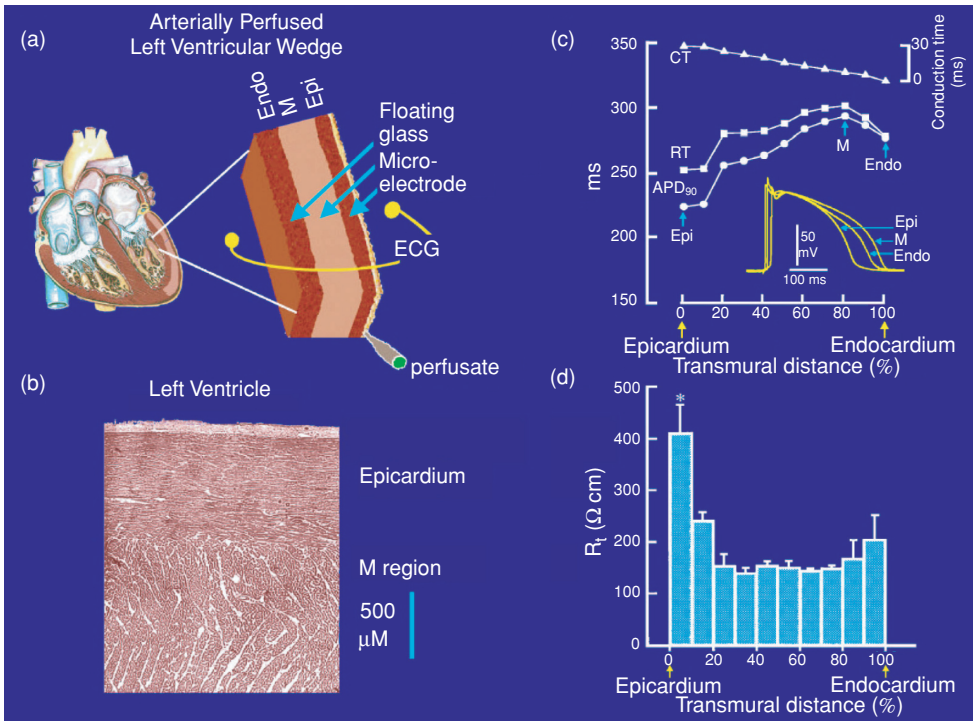

Figure 1.2 Transmural distribution of action potential duration and tissue resistivity across the ventricular wall. (a) Schematic diagram of the coronary-perfused canine LV wedge preparation. Transmembrane action potentials are recorded simultaneously from epicardial (Epi), M region (M), and endocardial (Endo) sites using three floating microelectrodes. A transmural ECG is recorded along the same transmural axis across the bath, registering the entire field of the wedge. (b) Histology of a transmural slice of the left ventricular wall near the epicardial border. The region of sharp transition of cell orientation coincides with the region of high tissue resistivity depicted in Panel (d) and the region of sharp transition of action potential duration illustrated in Panel (c). (c) Distribution of conduction time (CT), APD_{90}, and repolarization time (RT = APD_{90} + CT) in a canine left ventricular wall wedge preparation paced at BCL of 2000 milliseconds. A sharp transition of APD_{90} is present between epicardium and subepicardium. Epi: epicardium; M: M cell; Endo: endocardium. RT: repolarization time; CT: conduction time. (d) Distribution of total tissue resistivity (R_t) across the canine left ventricular wall. Transmural distances at 0% and 100% represent epicardium and endocardium, respectively. * $P < 0.01$ compared with R_t at mid-wall. Tissue resistivity increases most dramatically between deep subepicardium and epicardium. Error bars represent SEM ($n = 5$). From [21,23], with permission.

resistivity in this region [23], which may be related to the sharp transition in cell orientation in this region as well as to reduced expression of connexin43 [45,46], which is principally responsible for intracellular communication in ventricular myocardium. Moreover, LeGrice et al. [47] have shown that the density of collagen is heterogeneously distributed across the ventricular wall. A greater density of collagen in the deep subepicardium may also contribute to the resistive barrier in this region of the wall, limiting the degree of electrotonic interaction between myocardial layers. The degree of electrotonic coupling, together with the intrinsic differences APD, contribute to TDR in the ventricular myocardium [48].

The ionic bases for these features of the M cell include the presence of a smaller slowly activating delayed rectifier current (I_{Ks}) [30], a larger late sodium current (late I_{Na}) [49], and a larger Na–Ca exchange current ($I_{Na–Ca}$) [50]. In the canine heart, the rapidly activating delayed rectifier (I_{Kr}) and the inward rectifier (I_{K1}) currents are similar in the three transmural cell types. Transmural and apico-basal differences in the density of I_{Kr} channels have been described in the ferret heart [51]. I_{Kr} message and channel protein are much larger in

the ferret epicardium. I_{Ks} is larger in M cells isolated from the right versus left ventricles of the dog [12]. These ionic distinctions sensitize the M cells to a variety of pharmacological agents. Agents that block the rapidly activating delayed rectifier current (I_{Kr}), I_{Ks}, or that increase calcium channel current (I_{Ca}) or late I_{Na}, generally produce a much greater prolongation of the APD of the M cell than of epicardial or endocardial cells leading to amplification of TDR.

Amplification of transmural heterogeneities normally present in the early and late phases of the action potential can lead to the development of a variety of arrhythmias, including Brugada, long-QT, and short-QT syndromes as well as catecholaminergic ventricular tachycardia (VT).

Brugada syndrome

The Brugada syndrome is an inherited primary electrical disease in which amplification of TDR is believed to lead to the development of polymorphic VT and sudden cardiac death [52]. The Brugada ECG is characterized by an elevated ST segment or J wave appearing in the right precordial leads (V1–V3), often followed by a negative T wave. First described in 1992, the syndrome is associated with a high incidence of sudden cardiac death secondary to a rapid polymorphic VT or ventricular fibrillation (VF) [53]. The ECG characteristics of the Brugada syndrome are dynamic and often concealed, but can be unmasked by potent sodium channel blockers such as ajmaline, flecainide, procainamide, disopyramide, propafenone, and pilsicainide [54–56].

The Brugada syndrome (BrS) is associated with mutations in *SCN5A*, the gene that encodes the α subunit of the cardiac sodium channel, in approximately 15% of probands [57]. Over one hundred mutations in *SCN5A* have been linked to the syndrome in recent years (see [58] for references; also see http://www.fsm.it/cardmoc). Only a fraction of these mutations have been studied in expression systems and shown to result in loss of function of sodium channel activity. Weiss et al. [59] described a second locus on chromosome 3, close to but distinct from *SCN5A*, linked to the syndrome in a large pedigree in which the syndrome is associated with progressive conduction disease, a low sensitivity to procainamide, and a relatively good prognosis. The gene was recently identified in a preliminary report as the *Glycerol-3-Phosphate Dehydrogenase 1-Like* (*GPD1L*) gene and the mutation in *GPD1L* was shown to result in a reduction of I_{Na} [60].

The third and fourth genes associated with the Brugada syndrome were recently identified and shown to encode the α1 (*CACNA1C*) and β (*CACNB2b*) subunits of the L-type cardiac calcium channel. Mutations in the α and β subunits of the calcium channel also lead to a shorter than normal QT interval, in some cases creating a new clinical entity consisting of a combined Brugada/short-QT syndrome [61].

Several experimental models of the BrS have been developed using the right coronary-perfused right ventricular wedge preparation [62–66]. The available data point to amplification of heterogeneities intrinsic to the early phases (phase 1-mediated notch) of the action potential of cells residing in different layers of the right ventricular wall of the heart as the basis for the development of extrasystolic activity and polymorphic VT in BrS (Figure 1.3). Rebalancing of the currents active at the end of phase 1 can lead to accentuation of the action potential notch in right ventricular epicardium, which is responsible for the augmented J wave and ST segment elevation associated with the Brugada syndrome (see [52,67] for references). Under physiologic conditions, the ST segment is isoelectric due to the absence of major transmural voltage gradients at the level of the action potential plateau. Accentuation of the right ventricular action potential notch under pathophysiological conditions leads to exaggeration of transmural voltage gradients and thus to accentuation of the J wave or to an elevation of the J point (Figure 1.3). If the epicardial action potential continues to repolarize before that of endocardium, the T wave remains positive, giving rise to a saddleback configuration of the ST segment elevation. Further accentuation of the notch is accompanied by a prolongation of the epicardial action potential causing it to repolarize after endocardium, thus leading to inversion of the T wave [62,63]. Despite the appearance of a typical Brugada ECG, accentuation of the RV epicardial action potential (AP) notch alone does not give rise to an arrhythmogenic substrate. The arrhythmogenic substrate may develop with a further shift in the balance of current leading to loss of the action potential dome at

some epicardial sites but not others. A steep gradient of TDR develops as a consequence, creating a vulnerable window, which when captured by a premature extrasystole can trigger a reentrant arrhythmia. Because loss of the action potential dome in epicardium is generally heterogeneous, epicardial dispersion of repolarization develops as well. Propagation of the action potential dome from sites at which it is maintained to sites at which it is lost causes local reexcitation via phase 2 reentry, leading to the development of a closely coupled extrasystole capable of capturing the vulnerable window across the ventricular wall, thus triggering a circus movement reentry in the form of VT/VF (Figures 1.3 and 1.4) [62,68,69]. The polymorphic VT may start in epicardium reentry, but quickly shifts to an intramural reentry before self-terminating or deteriorating to VF [69].

Evidence in support of these hypotheses derives from experiments involving the arterially perfused right ventricular wedge preparation [62,63,66,69, 70] and from studies in which monophasic action potential (MAP) electrodes were positioned on the epicardial and endocardial surfaces of the right ventricular outflow tract (RVOT) in patients with the Brugada syndrome [71,72].

Long-QT syndrome

The long-QT syndromes (LQTS) are phenotypically and genotypically diverse, but have in common the appearance of a long QT interval in the ECG, an atypical polymorphic VT known as Torsade de Pointes (TdP), and, in many but not all cases, a relatively high risk for sudden cardiac death [73–75]. Ten genotypes of the congenital LQTS have been identified. The identified syndromes are distinguished by mutations in at least eight different ion channel genes, a structural anchoring protein, and a caveolin protein located on chromosomes 3, 4, 6, 7, 11, 17, and 21 (Table 1.1) [76–81].

The most recent genes associated with LQTS are *CAV3* which encodes caveolin-3 and *SCN4B* which encodes $Na_V B4$, an auxiliary subunit of the cardiac sodium channel. Caveolin-3 spans the plasma membrane twice, forming a hairpin structure on the surface, and is the main constituent of caveolae, small invaginations in the plasma membrane. Mutations both in *CAV3* and in *SCNB4* produce a gain in function in late I_{Na}, causing an LQT3-like phenotype [82,83].

LQTS shows both autosomal recessive and autosomal dominant patterns of inheritance: (1) a rare autosomal recessive disease associated with deafness (Jervell and Lange-Nielsen), caused by two genes that encode for the slowly activating delayed rectifier potassium channel (*KCNQ1* and *KCNE1*); and (2) a much more common autosomal dominant form known as the Romano–Ward syndrome, caused by mutations in 10 different genes (Table 1.1). Eight of the 10 genes encode cardiac ion channels.

Acquired LQTS refers to a QT prolongation caused by exposure to drugs that prolong the duration of the ventricular action potential [84] or QT prolongation secondary to cardiomyopathies including dilated or hypertrophic cardiomyopathy, as well as to abnormal QT prolongation associated with bradycardia or electrolyte imbalance [85–89]. The acquired form of the disease is far more prevalent than the congenital form and in some cases may have a genetic predisposition [90].

Amplification of spatial dispersion of repolarization within the ventricular myocardium has been identified as the principal arrhythmogenic substrate in both acquired and congenital LQTS. The amplification of spatial dispersion of refractoriness can take the form of an increase in transmural, transseptal, or apico-basal dispersion of repolarization. This exaggerated intrinsic heterogeneity together with EAD- and DAD-induced triggered activity, both caused by reduction in net repolarizing current, underlie the substrate and trigger for the development of TdP arrhythmias observed under LQTS conditions [91,92]. Models of the LQT1, LQT2, and LQT3 forms of the LQTS have been developed using the canine arterially perfused left ventricular wedge preparation (Figure 1.5) [93]. These models suggest that in these three forms of LQTS, preferential prolongation of the M cell APD leads to an increase in the QT interval as well as an increase in TDR, which contributes to the development of spontaneous as well as stimulation-induced TdP via an intramural reentry mechanism (Figure 1.6) [35,40,94–97]. The spatial dispersion of repolarization is further exaggerated by sympathetic influences in LQT1 and LQT2, accounting for the great sensitivity of patients with these genotypes to adrenergic stimuli (Figures 1.5 and 1.6).

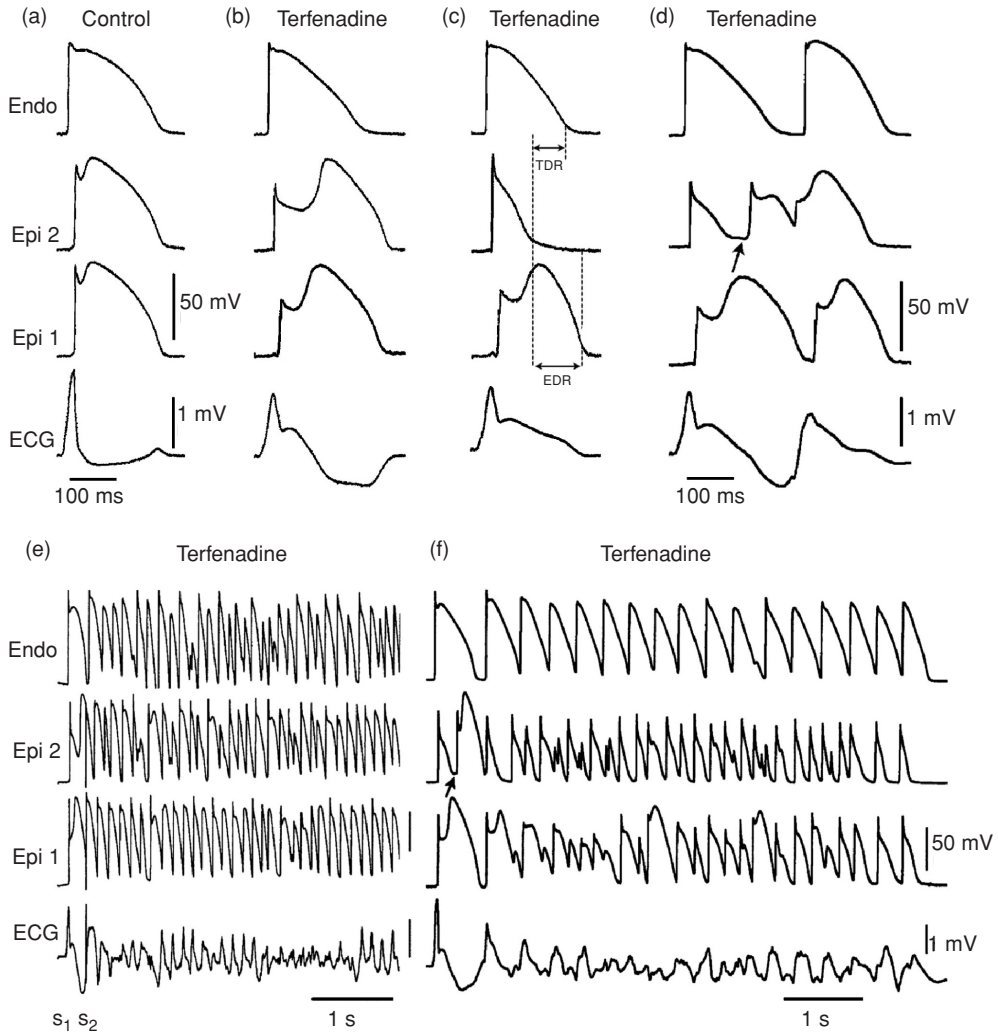

Figure 1.3 Cellular basis for electrocardiographic and arrhythmic manifestation of Brugada syndrome. Each panel shows transmembrane action potentials from one endocardial (top) and two epicardial sites together with a transmural ECG recorded from a canine coronary-perfused right ventricular wedge preparation. (a) Control (BCL 400 ms). (b) Combined sodium and calcium channel block with terfenadine (5 μM) accentuates the epicardial action potential notch, creating a transmural voltage gradient that manifests as an ST segment elevation or exaggerated J wave in the ECG. (c) Continued exposure to terfenadine results in all-or-none repolarization at the end of phase 1 at some epicardial sites but not others, creating a local epicardial dispersion of repolarization (EDR) as well as a transmural dispersion of repolarization (TDR). (d) Phase 2 reentry occurs when the epicardial action potential dome propagates from a site where it is maintained to regions where it has been lost, giving rise to a closely coupled extrasystole. (e) Extrastimulus (S1 – S2 = 250 ms) applied to epicardium triggers a polymorphic VT. (f) Phase 2 reentrant extrasystole triggers a brief episode of polymorphic VT. (Modified from Ref. [63], with permission).

Voltage gradients that develop as a result of the different time course of repolarization of phases 2 and 3 in the three cell types give rise to opposing voltage gradients on either side of the M region, which are in part responsible for the inscription of the T wave [44]. In the case of an upright T wave, the epicardial response is the earliest to repolarize and the M cell action potential is the latest. Full repolarization of the epicardial action potential coincides with the peak of the T wave and repolarization of

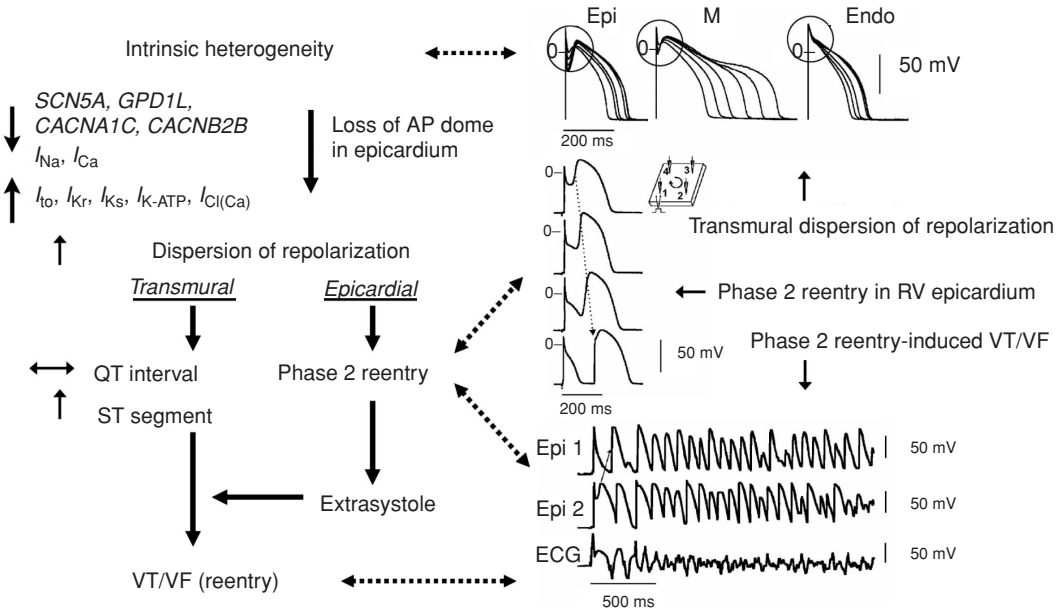

Figure 1.4 Proposed mechanism for the Brugada syndrome. A shift in the balance of currents serves to amplify existing heterogeneities by causing loss of the action potential dome at some epicardial, but not endocardial sites. A vulnerable window develops as a result of the dispersion of repolarization and refractoriness within epicardium as well as across the wall. Epicardial dispersion leads to the development of phase 2 reentry, which provides the extrasystole that captures the vulnerable window and initiates VT/VF via a circus movement reentry mechanism. Modified from [128], with permission.

the M cells is coincident with the end of the T wave. The duration of the M cell action potential therefore determines the QT interval, whereas the duration of the epicardial action potential determines the QT_{peak} interval. The interval between the peak and end of the T wave (T_{peak}–T_{end} interval) in precordial ECG leads is suggested to provide an index of TDR [2]. Recent studies provide guidelines for the estimation of TDR in the case of more complex T waves, including negative, biphasic, and triphasic T waves [98]. In these cases, the interval from the nadir of the first component of the T wave to the end of the T wave provides an approximation of TDR.

Because the precordial leads (V1–V6) are designed to view the electrical field across the ventricular wall, T_{peak}–T_{end} is the most representative of TDR in these leads. T_{peak}–T_{end} intervals measured in the limb leads are unlikely to provide an index of TDR, but may provide a measure of global dispersion within the heart [99,100]. Because TDR can vary dramatically in different regions of the heart, it is inadvisable to average T_{peak}–T_{end} among all or several leads [100]. Because LQTS is principally a left ventricular disorder, TDR is likely to be greatest in the left ventricular wall or septum and thus be best reflected in left precordial leads or V3, respectively [101]. In contrast, because Brugada syndrome is a right ventricular disorder, TDR is greatest in the right ventricular free wall and thus is best reflected in the right precordial leads [102].

T_{peak}–T_{end} interval does not provide an absolute measure of transmural dispersion *in vivo* [100], although changes in this parameter are thought to reflect changes in spatial dispersion of repolarization, including TDR, and thus may be prognostic of arrhythmic risk under a variety of conditions [103–108]. Takenaka et al. [107] recently demonstrated exercise-induced accentuation of the T_{peak}–T_{end} interval in LQT1 patients, but not LQT2. These observations coupled with those of Schwartz et al. [109], demonstrating an association between exercise and risk for TdP in LQT1 but not LQT2 patients, once again point to the potential value of T_{peak}–T_{end} in forecasting risk for the development of TdP. Direct evidence in support of T_{peak}–T_{end} measured in V5 as an index to predict TdP in patients with LQTS was provided by Yamaguchi and co-workers [101]. These authors concluded that T_{peak}–T_{end} is

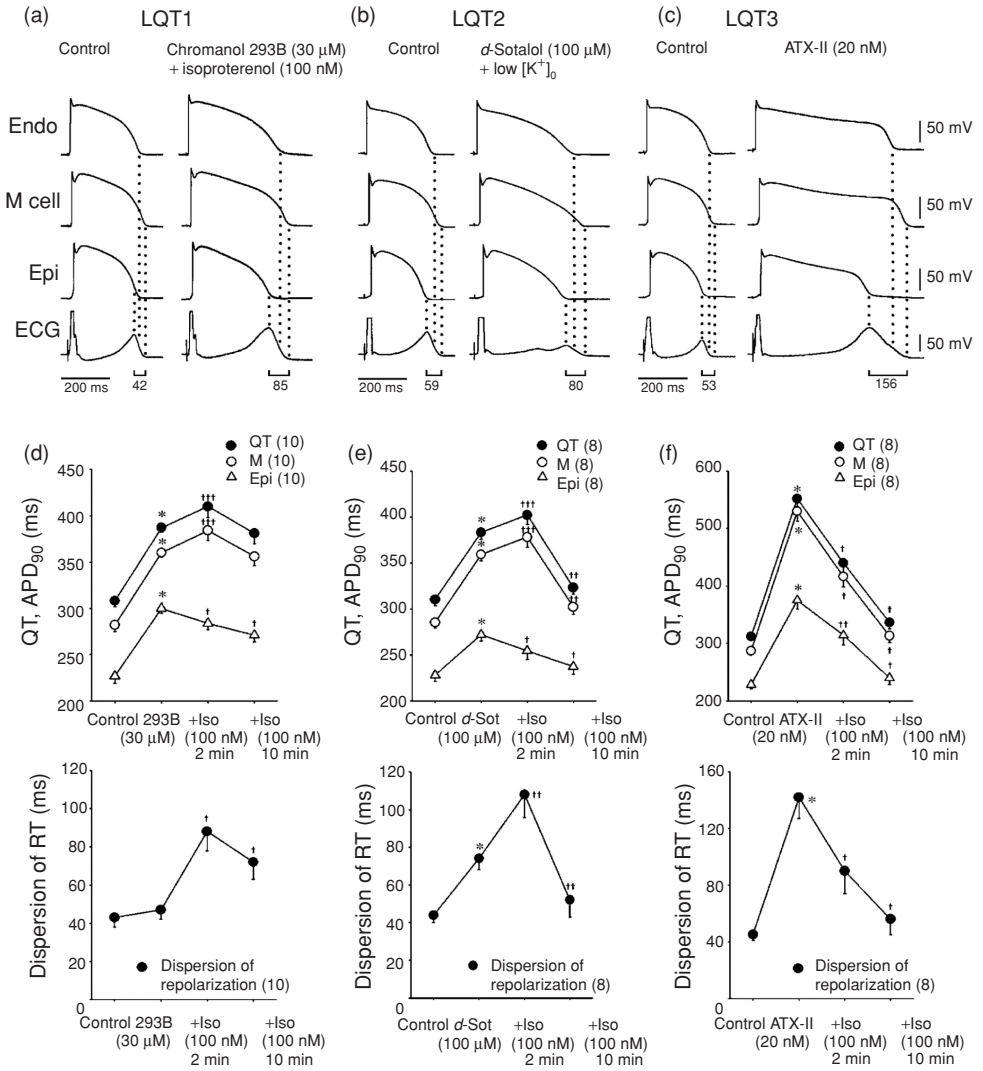

Figure 1.5 LQT1, LQT2, and LQT3 models of LQTS. Panels (a)–(c) show action potentials recorded simultaneously from endocardial (Endo), M, and epicardial (Epi) sites of arterially perfused canine left ventricular wedge preparations together with a transmural ECG. BCL = 2000 milliseconds. Transmural dispersion of repolarization across the ventricular wall, defined as the difference in the repolarization time between M and epicardial cells, is denoted below the ECG traces. LQT1 model was mimicked using Isoproterenol + chromanol 293B − an I_{Ks} blocker. LQT2 was created using the I_{Kr} blocker *d*-sotalol + low $[K^+]_o$. LQT3 was mimicked using the sea anemone toxin ATX-II to augment late I_{Na}. Panels (d)–(f): Effect of isoproterenol in the LQT1, LQT2, and LQT3 models. In LQT1, isoproterenol (Iso) produces a persistent prolongation both of the APD_{90} of the M cell and of the QT interval (at both 2 and 10 min), whereas the APD_{90} of the epicardial cell is always abbreviated, resulting in a persistent increase in TDR (d). In LQT2, isoproterenol initially prolongs (2 min) and then abbreviates the QT interval and the APD_{90} of the M cell to the control level (10 min), whereas the APD_{90} of epicardial cell is always abbreviated, resulting in a transient increase in TDR (e). In LQT3, isoproterenol produced a persistent abbreviation of the QT interval and the APD_{90} of both M and epicardial cells (at both 2 and 10 min), resulting in a persistent decrease in TDR (f). $*P < 0.0005$ versus Control; $\dagger P < 0.0005$, $\dagger\dagger P < 0.005$, $\dagger\dagger\dagger P < 0.05$, versus 293B, *d*-Sotalol (*d*-Sot), or ATX-II. (Modified from references [35,40,94] with permission).

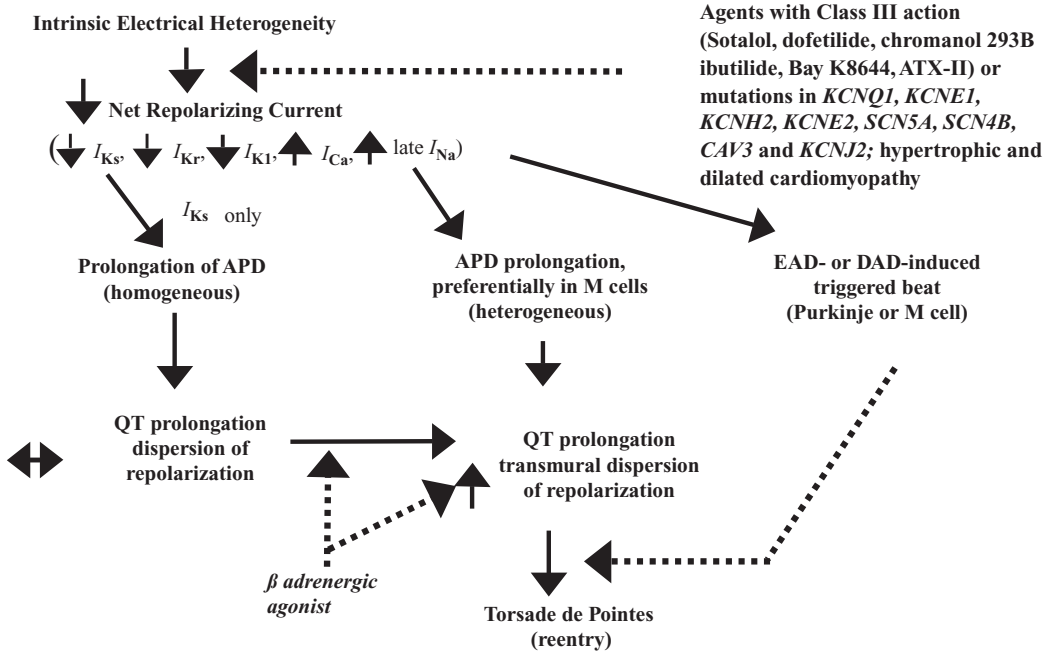

Figure 1.6 Proposed cellular mechanism for the development of Torsade de Pointes in the long-QT syndromes.

more valuable than QTc and QT dispersion as a predictor of TdP in patients with acquired LQTS. Shimizu et al. [106] demonstrated that T_{peak}–T_{end}, but not QTc, predicted sudden cardiac death in patients with hypertrophic cardiomyopathy. Most recently, Watanabe et al. [108] demonstrated that prolonged T_{peak}–T_{end} is associated with inducibility as well as spontaneous development of VT in high-risk patients with organic heart disease. Evidence in support of a significant correlation between T_{peak}–T_{end}, and T_{peak}–T_{end} dispersion and the occurrence of life-threatening arrhythmic events in patients with BrS was recently presented by Castro and co-workers [102].

The accumulated data support the hypothesis that TDR rather than QT prolongation underlies the principal substrate for the development of TdP [91,110–113]. Our working hypothesis for the development of LQTS-related TdP presumes the presence of electrical heterogeneity in the form of TDR under baseline conditions and the amplification of TDR by agents that reduce net repolarizing current via a reduction either in I_{Kr} or in I_{Ks} or augmentation either of I_{Ca} or of late I_{Na} (Figure 1.6). Conditions leading to a reduction in I_{Kr} or augmentation of late I_{Na} produce a preferential prolongation of the M cell action potential. As a consequence, the QT interval prolongs and is accompanied by a dramatic increase in TDR, thus creating a vulnerable window for the development of reentry. The reduction in net repolarizing current also predisposes to the development of EAD-induced triggered activity in M and Purkinje cells, which provide the extrasystole that triggers TdP when it falls within the vulnerable period. β Adrenergic agonists further amplify transmural heterogeneity (transiently) in the case of I_{Kr} block, but reduce it in the case of sodium channel current (I_{Na}) agonists [33,94].

Agents that selectively block I_{Kr} for increase in late I_{Na} always produced a preferential prolongation of the M cell action potential and thus augment TDR. However, not all agents that prolong the QT interval increase TDR. Amiodarone, a potent antiarrhythmic agent used in the management of both atrial and ventricular arrhythmias, is rarely associated with TdP. Chronic administration of amiodarone produces a greater prolongation of APD in epicardium and endocardium, but less of an increase, or even a decrease at slow rates, in the M region, thereby reducing TDR [114]. In a dog model of chronic complete atrioventricular block and acquired LQTS, 6 weeks of amiodarone was shown to

produce a major QT prolongation without producing TdP. In contrast, after 6 weeks of dronedarone, TdP occurred in 4 of 8 dogs with the highest spatial dispersion of repolarization (105 ± 20 ms) [115].

Another example of an agent that prolongs the QT interval but does increase TDR is sodium pentobarbital. Indeed, sodium pentobarbital has been shown to produce a dose-dependent prolongation of the QT interval, which is accompanied by a reduction in TDR [39]. TdP is not found to happen under these conditions nor can it be induced with programmed electrical stimulation. Amiodarone and pentobarbital have in common the ability to block I_{Ks}, I_{Kr}, and late I_{Na}. This combination produces a preferential prolongation of the APD of epicardium and endocardium so that the QT interval is prolonged, but TDR is actually reduced and TdP does not develop. Cisapride is another agent that blocks both inward and outward currents. In the canine left ventricular wedge preparation, cisapride produces a biphasic dose-dependent prolongation of the QT interval and TDR. TDR peaks at 0.2 μM, and it is only at this concentration that TdP is observed. Higher concentrations of cisapride lead to an abbreviation of TDR and elimination of TdP, even though QT is further prolonged [113]. This finding suggests that the spatial dispersion of repolarization is more important than the prolongation of the QT interval in determining the substrate for TdP.

Chromanol 293B, a blocker of I_{Ks}, also increases QT without augmenting TDR. Chromanol 293B prolongs APD of the three cell types homogeneously, neither increasing TDR nor widening the T wave. TdP is never observed under these conditions. The addition of β adrenergic agonist, however, abbreviates the APD of epicardial and endocardial cells but not that of the M cell, resulting in a marked accentuation of TDR and the development of TdP [94].

Short-QT syndrome

The short-QT syndrome (SQTS) is characterized by a QTc ≤360 milliseconds and high incidence of VT/VF in infants, children and young adults [116–118]. The first genetic defect responsible for this familial syndrome (*SQTS1*) involved two different missense mutations that resulted in the same amino acid substitution of lysine for an asparagine in position 588 of *HERG* (*N588K*). The mutation caused a gain of function in the rapidly activating delayed rectifier channel, I_{Kr} [119]. A second gene, reported by Bellocq et al. [120] (*SQTS2*), involved a missense mutation in *KCNQ1* (*KvLQT1*), which caused a gain of function in I_{Ks}. A third gene (*SQTS3*) involved *KCNJ2*, the gene that encodes the inward rectifier channel. Mutations in *KCNJ2* caused a gain of function in I_{K1}, leading to an abbreviation of QT interval. SQT3 is associated with QTc interval of <330 milliseconds, not quite as short as SQT1, and SQT2. Two additional genes recently linked to SQTS encode the α1 (*CACNA1C*) and β (*CACNB2b*) subunits of the L-type cardiac calcium channel. SQT4, caused by mutations in the α subunit of calcium channel, have been shown to lead to the QT interval <360 milliseconds, whereas SQT5 caused by mutations in the β subunit of the calcium channel is characterized by QT intervals of 330–360 milliseconds [61]. Mutations in the α and β subunits of the calcium channel may also lead to ST segment elevation, creating a combined Brugada/ SQTS [61].

In SQT1, 2, and 3, the ECG commonly displays tall peaked symmetrical T waves secondary to acceleration of phase 3 repolarization. An augmented T_{peak}–T_{end} interval is associated with this electrocardiographic feature of the syndrome, suggesting that TDR is significantly increased (Figure 1.7). A left ventricular wedge model of the SQTS developed using the ATP-sensitive potassium channel ($I_{K\text{-}ATP}$) opener, pinacidil, to augment outward repolarizing current also demonstrated an increase in TDR due to a preferential abbreviation of endocardial/M cell action potential duration. The increase in TDR coupled with the abbreviation of QT and refractoriness permitted the development of intramural reentry, giving rise to a rapid polymorphic VT [121]. The increase in TDR was further accentuated by isoproterenol, leading to easier induction and more persistent VT/VF. Of note, an increase in TDR to values greater than 55 milliseconds was associated with inducibility of VT/VF. In LQTS models, a TDR of >90 milliseconds is required to induce TdP. The easier inducibility in SQTS is due to the reduction in the wavelength (refractory period × conduction velocity) of the reentrant circuit, which reduces the pathlength required for maintenance of reentry [121].

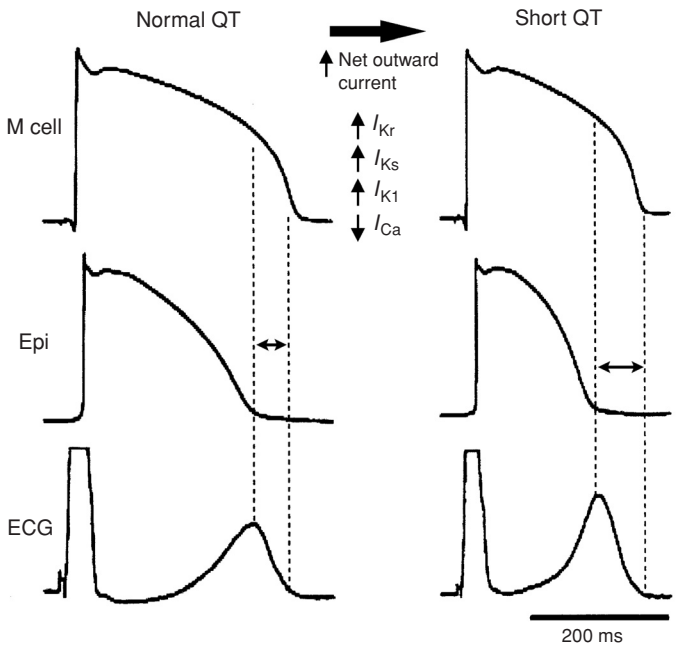

Figure 1.7 Proposed mechanism for arrhythmogenesis in the short-QT syndrome. An increase in net outward current due to a reduction in late inward current or augmentation of outward repolarizing current serves to abbreviate action potential duration heterogeneously leading to an amplification of transmural dispersion of repolarization and the creation of a vulnerable window for the development of reentry. Reentry is facilitated both by the increase in TDR and abbreviation of refractoriness.

Intramural reentry secondary to amplification of TDR as a common denominator in channelopathy-induced sudden cardiac death

The three inherited sudden cardiac death syndromes reviewed differ with respect to the characteristics of the QT interval (Figure 1.8). In LQTS, QT increases as a function of disease or drug concentration. In the Brugada syndrome it remains largely unchanged and in the SQTS QT interval decreases as a function of either disease or drug. What these three syndromes have in common is an amplification of TDR, which results in the development of polymorphic VT and fibrillation when dispersion of

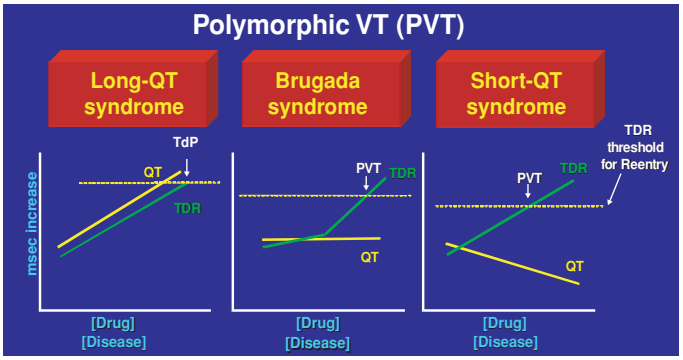

Figure 1.8 The role of transmural dispersion of repolarization (TDR) in channelopathy-induced sudden cardiac death. In the long-QT syndrome, QT increases as a function of disease or drug concentration. In the Brugada syndrome it remains largely unchanged and in the short-QT syndrome QT interval decreases as a function of disease or drug. The three syndromes have in common the ability to amplify TDR, which results in the development of TdP when dispersion reaches the threshold for reentry. The threshold for reentry decreases as APD and refractoriness are reduced. Modified from [129], with permission.

repolarization and refractoriness reaches the threshold for reentry. When polymorphic VT occurs in the setting of long QT, we refer to it as TdP. The threshold for reentry decreases as APD and refractoriness are reduced and the pathlength required for establishing a reentrant wave is progressively reduced.

Conclusion

Amplification of spatial dispersion of refractoriness in ventricular myocardium, particularly when due to augmentation of TDR, can predispose to the development of potentially lethal reentrant arrhythmias in a variety of ion channelopathies including long-QT, short-QT, and Brugada syndromes. These principles apply to arrhythmogenesis associated with both hypertrophic and dilated cardiomyopathies [122–125] as well as some arrhythmias associated with ischemia and reperfusion [126,127].

References

1 Antzelevitch C, Sicouri S, Litovsky SH, et al. Heterogeneity within the ventricular wall. Electrophysiology and pharmacology of epicardial, endocardial, and M cells. Circ Res 1991;69:1427–1449.

2 Antzelevitch C, Shimizu W, Yan GX, et al. The M cell: its contribution to the ECG and to normal and abnormal electrical function of the heart. J Cardiovasc Electrophysiol 1999;10:1124–1152.

3 Litovsky SH, Antzelevitch C. Transient outward current prominent in canine ventricular epicardium but not endocardium. Circ Res 1988;62:116–126.

4 Liu DW, Gintant GA, Antzelevitch C. Ionic bases for electrophysiological distinctions among epicardial, midmyocardial, and endocardial myocytes from the free wall of the canine left ventricle. Circ Res 1993;72:671–687.

5 Furukawa T, Myerburg RJ, Furukawa N, Bassett AL, Kimura S. Differences in transient outward currents of feline endocardial and epicardial myocytes. Circ Res 1990;67:1287–1291.

6 Fedida D, Giles WR. Regional variations in action potentials and transient outward current in myocytes isolated from rabbit left ventricle. J Physiol (Lond) 1991;442:191–209.

7 Clark RB, Bouchard RA, Salinas-Stefanon E, Sanchez-Chapula J, Giles WR. Heterogeneity of action potential waveforms and potassium currents in rat ventricle. Cardiovasc Res 1993;27:1795–1799.

8 Campbell DL, Rasmusson RL, Qu YH, Strauss HC. The calcium-independent transient outward potassium current in isolated ferret right ventricular myocytes. I. Basic characterization and kinetic analysis. J Gen Physiol 1993;101:571–601.

9 Wettwer E, Amos GJ, Posival H, Ravens U. Transient outward current in human ventricular myocytes of subepicardial and subendocardial origin. Circ Res 1994;75:473–482.

10 Nabauer M, Beuckelmann DJ, Uberfuhr P, Steinbeck G. Regional differences in current density and rate-dependent properties of the transient outward current in subepicardial and subendocardial myocytes of human left ventricle. Circulation 1996;93:168–177.

11 Di Diego JM, Sun ZQ, Antzelevitch C. I_{to} and action potential notch are smaller in left vs. right canine ventricular epicardium. Am J Physiol 1996;271:H548–H561.

12 Volders PG, Sipido KR, Carmeliet E, Spatjens RL, Wellens HJ, Vos MA. Repolarizing K^+ currents ITO1 and IKs are larger in right than left canine ventricular midmyocardium. Circulation 1999;99:206–210.

13 Wang HS, Cohen IS. Calcium channel heterogeneity in canine left ventricular myocytes. J Physiol 2003;547:825–833.

14 Cordeiro JM, Greene L, Heilmann C, Antzelevitch D, Antzelevitch C. Transmural heterogeneity of calcium activity and mechanical function in the canine left ventricle. Am J Physiol Heart Circ Physiol 2004;286:H1471–H1479.

15 Banyasz T, Fulop L, Magyar J, Szentandrassy N, Varro A, Nanasi PP. Endocardial versus epicardial differences in L-type calcium current in canine ventricular myocytes studied by action potential voltage clamp. Cardiovasc Res 2003;58:66–75.

16 Takano M, Noma A. Distribution of the isoprenaline-induced chloride current in rabbit heart. Pflugers Arch 1992;420:223–226.

17 Zygmunt AC. Intracellular calcium activates chloride current in canine ventricular myocytes. Am J Physiol 1994;267:H1984–H1995.

18 Sicouri S, Antzelevitch C. A subpopulation of cells with unique electrophysiological properties in the deep subepicardium of the canine ventricle. The M cell. Circ Res 1991;68:1729–1741.

19 Anyukhovsky EP, Sosunov EA, Gainullin RZ, Rosen MR. The controversial M cell. J Cardiovasc Electrophysiol 1999;10:244–260.

20 Anyukhovsky EP, Sosunov EA, Rosen MR. Regional differences in electrophysiologic properties of epicardium, midmyocardium and endocardium: *In vitro* and *in vivo* correlations. Circulation 1996;94:1981–1988.

21 Antzelevitch C, Dumaine R. Electrical heterogeneity in the heart: physiological, pharmacological and clinical implications. In: Page E, Fozzard HA, Solaro RJ, eds. *Handbook of Physiology. Section 2: The Cardiovascular System.* New York: Oxford University Press; 2001:654–692.

22 Burashnikov A, Antzelevitch C. Differences in the electrophysiologic response of four canine ventricular cell types to a_1-adrenergic agonists. Cardiovasc Res 1999;43:901–908.

23 Yan GX, Shimizu W, Antzelevitch C. Characteristics and distribution of M cells in arterially-perfused

canine left ventricular wedge preparations. Circulation 1998;98:1921–1927.
24 Sicouri S, Antzelevitch C. Electrophysiologic characteristics of M cells in the canine left ventricular free wall. J Cardiovasc Electrophysiol 1995;6:591–603.
25 Sicouri S, Fish J, Antzelevitch C. Distribution of M cells in the canine ventricle. J Cardiovasc Electrophysiol 1994;5:824–837.
26 Antzelevitch C, Sicouri S. Clinical relevance of cardiac arrhythmias generated by afterdepolarizations. Role of M cells in the generation of U waves, triggered activity and torsade de pointes. J Am Coll Cardiol 1994;23:259–277.
27 Stankovicova T, Szilard M, De Scheerder I, Sipido KR. M cells and transmural heterogeneity of action potential configuration in myocytes from the left ventricular wall of the pig heart. Cardiovasc Res 2000;45:952–960.
28 Sicouri S, Antzelevitch C. Drug-induced afterdepolarizations and triggered activity occur in a discrete subpopulation of ventricular muscle cell (M cells) in the canine heart: Quinidine and Digitalis. J Cardiovasc Electrophysiol 1993;4:48–58.
29 Drouin E, Charpentier F, Gauthier C, Laurent K, Le Marec H. Electrophysiological characteristics of cells spanning the left ventricular wall of human heart: evidence for the presence of M cells. J Am Coll Cardiol 1995;26:185–192.
30 Liu DW, Antzelevitch C. Characteristics of the delayed rectifier current (IKr and IKs) in canine ventricular epicardial, midmyocardial, and endocardial myocytes. Circ Res 1995;76:351–365.
31 Weissenburger J, Nesterenko VV, Antzelevitch C. Transmural heterogeneity of ventricular repolarization under baseline and long QT conditions in the canine heart *in vivo*: Torsades de Pointes develops with halothane but not pentobarbital anesthesia. J Cardiovasc Electrophysiol 2000;11:290–304.
32 Sicouri S, Quist M, Antzelevitch C. Evidence for the presence of M cells in the guinea pig ventricle. J Cardiovasc Electrophysiol 1996;7:503–511.
33 Li GR, Feng J, Yue L, Carrier M. Transmural heterogeneity of action potentials and Ito1 in myocytes isolated from the human right ventricle. Am J Physiol 1998;275:H369–H377.
34 Rodriguez-Sinovas A, Cinca J, Tapias A, Armadans L, Tresanchez M, Soler-Soler J. Lack of evidence of M-cells in porcine left ventricular myocardium. Cardiovasc Res 1997;33:307–313.
35 Shimizu W, Antzelevitch C. Sodium channel block with mexiletine is effective in reducing dispersion of repolarization and preventing Torsade de Pointes in LQT2 and LQT3 models of the long-QT syndrome. Circulation 1997;96:2038–2047.
36 El-Sherif N, Caref EB, Yin H, Restivo M. The electrophysiological mechanism of ventricular arrhythmias in the long QT syndrome: tridimensional mapping of activation and recovery patterns. Circ Res 1996;79:474–492.
37 Weirich J, Bernhardt R, Loewen N, Wenzel W, Antoni H. Regional- and species-dependent effects of K^+-channel blocking agents on subendocardium and mid-wall slices of human, rabbit, and guinea pig myocardium [Abstract]. Pflugers Arch 1996;431:R 130.
38 Burashnikov A, Antzelevitch C. Acceleration-induced action potential prolongation and early afterdepolarizations. J Cardiovasc Electrophysiol 1998;9:934–948.
39 Shimizu W, McMahon B, Antzelevitch C. Sodium pentobarbital reduces transmural dispersion of repolarization and prevents torsade de pointes in models of acquired and congenital long QT syndrome. J Cardiovasc Electrophysiol 1999;10:156–164.
40 Shimizu W, Antzelevitch C. Cellular basis for the ECG features of the LQT1 form of the long QT syndrome: effects of b-adrenergic agonists and antagonists and sodium channel blockers on transmural dispersion of repolarization and Torsade de Pointes. Circulation 1998;98:2314–2322.
41 Shimizu W, Antzelevitch C. Cellular and ionic basis for T-wave alternans under Long QT conditions. Circulation 1999;99:1499–1507.
42 Balati B, Varro A, Papp JG. Comparison of the cellular electrophysiological characteristics of canine left ventricular epicardium, M cells, endocardium and Purkinje fibres. Acta Physiol Scand 1998;164:181–190.
43 McIntosh MA, Cobbe SM, Smith GL. Heterogeneous changes in action potential and intracellular Ca^{2+} in left ventricular myocyte sub-types from rabbits with heart failure. Cardiovasc Res 2000;45:397–409.
44 Yan GX, Antzelevitch C. Cellular basis for the normal T wave and the electrocardiographic manifestations of the long QT syndrome. Circulation 1998;98:1928–1936.
45 Poelzing S, Akar FG, Baron E, Rosenbaum DS. Heterogeneous connexin43 expression produces electrophysiological heterogeneities across ventricular wall. Am J Physiol Heart Circ Physiol 2004;286:H2001–H2009.
46 Yamada KA, Kanter EM, Green KG, Saffitz JE. Transmural distribution of connexins in rodent hearts. J Cardiovasc Electrophysiol 2004;15:710–715.
47 LeGrice IJ, Smaill BH, Chai LZ, Edgar SG, Gavin JB, Hunter PJ. Laminar structure of the heart 1: cellular organization and connective tissue architecture in ventricular myocardium. Am J Physiol 1996;269:H571–H582.
48 Viswanathan PC, Rudy Y. Cellular arrhythmogenic effects of the congenital and acquired long QT syndrome in the heterogeneous myocardium. Circulation 2000;101:1192–1198.
49 Zygmunt AC, Eddlestone GT, Thomas GP, Nesterenko VV, Antzelevitch C. Larger late sodium conductance in M cells contributes to electrical heterogeneity in canine ventricle. Am J Physiol 2001;281:H689–H697.
50 Zygmunt AC, Goodrow RJ, Antzelevitch C. I(NaCa) contributes to electrical heterogeneity within the canine ventricle. Am J Physiol Heart Circ Physiol 2000;278:H1671–H1678.
51 Brahmajothi MV, Morales MJ, Reimer KA, Strauss HC. Regional localization of ERG, the channel protein

responsible for the rapid component of the delayed rectifier, K^+ current in the ferret heart. Circ Res 1997;81:128–135.
52 Antzelevitch C. Brugada syndrome. PACE 2006;29: 1130–1159.
53 Brugada P, Brugada J. Right bundle branch block, persistent ST segment elevation and sudden cardiac death: a distinct clinical and electrocardiographic syndrome: a multicenter report. J Am Coll Cardiol 1992;20:1391–1396.
54 Brugada R, Brugada J, Antzelevitch C, et al. Sodium channel blockers identify risk for sudden death in patients with ST-segment elevation and right bundle branch block but structurally normal hearts. Circulation 2000;101:510–515.
55 Shimizu W, Antzelevitch C, Suyama K, et al. Effect of sodium channel blockers on ST segment, QRS duration, and corrected QT interval in patients with Brugada syndrome. J Cardiovasc Electrophysiol 2000;11:1320–1329.
56 Priori SG, Napolitano C, Gasparini M, et al. Clinical and genetic heterogeneity of right bundle branch block and ST-segment elevation syndrome: a prospective evaluation of 52 families. Circulation 2000;102:2509–2515.
57 Chen Q, Kirsch GE, Zhang D, et al. Genetic basis and molecular mechanisms for idiopathic ventricular fibrillation. Nature 1998;392:293–296.
58 Antzelevitch C, Brugada P, Brugada J, Brugada R. *The Brugada Syndrome: From Bench to Bedside.* Oxford: Blackwell Futura; 2005.
59 Weiss R, Barmada MM, Nguyen T, et al. Clinical and molecular heterogeneity in the Brugada syndrome. A novel gene locus on chromosome 3. Circulation 2002;105:707–713.
60 London B, Sanyal S, Michalec M, et al. AB16-1: a mutation in the glycerol-3-phosphate dehydrogenase 1-like gene (GPD1L) causes Brugada syndrome [Abstract]. Heart Rhythm 2006;3:S32.
61 Antzelevitch C, Pollevick GD, Cordeiro JM, et al. Loss-of-function mutations in the cardiac calcium channel underlie a new clinical entity characterized by ST-segment elevation, short QT intervals, and sudden cardiac death. Circulation 2007;115:442–449.
62 Yan GX, Antzelevitch C. Cellular basis for the Brugada syndrome and other mechanisms of arrhythmogenesis associated with ST segment elevation. Circulation 1999;100:1660–1666.
63 Fish JM, Antzelevitch C. Role of sodium and calcium channel block in unmasking the Brugada syndrome. Heart Rhythm 2004;1:210–217.
64 Di Diego JM, Cordeiro JM, Goodrow RJ, et al. Ionic and cellular basis for the predominance of the Brugada syndrome phenotype in males. Circulation 2002;106:2004–2011.
65 Aiba T, Hidaka I, Shimizu W, et al. Steep repolarization gradient is required for development of phase 2 reentry and subsequent ventricular tachyarrhythmias in a model of the Brugada syndrome: high-resolution optical mapping study [Abstract]. Circulation 2004;110:III-318.
66 Morita H, Zipes DP, Morita ST, Wu J. Temperature modulation of ventricular arrhythmogenicity in a canine tissue model of Brugada syndrome. Heart Rhythm 2007;4:188–197.
67 Antzelevitch C. The Brugada syndrome: ionic basis and arrhythmia mechanisms. J Cardiovasc Electrophysiol 2001;12:268–272.
68 Lukas A, Antzelevitch C. Phase 2 reentry as a mechanism of initiation of circus movement reentry in canine epicardium exposed to simulated ischemia. Cardiovasc Res 1996;32:593–603.
69 Aiba T, Shimizu W, Hidaka I, et al. Cellular basis for trigger and maintenance of ventricular fibrillation in the Brugada syndrome model: high-resolution optical mapping study. J Am Coll Cardiol 2006;47:2074–2085.
70 Morita H, Zipes DP, Lopshire J, Morita ST, Wu J. T wave alternans in an in vitro canine tissue model of Brugada syndrome. Am J Physiol Heart Circ Physiol 2006;291:H421–H428.
71 Antzelevitch C, Brugada P, Brugada J, et al. Brugada syndrome. A decade of progress. Circ Res 2002;91:1114–1119.
72 Kurita T, Shimizu W, Inagaki M, et al. The electrophysiologic mechanism of ST-segment elevation in Brugada syndrome. J Am Coll Cardiol 2002;40:330–334.
73 Schwartz PJ. The idiopathic long QT syndrome: progress and questions. Am Heart J 1985;109:399–411.
74 Moss AJ, Schwartz PJ, Crampton RS, et al. The long QT syndrome: prospective longitudinal study of 328 families. Circulation 1991;84:1136–1144.
75 Zipes DP. The long QT interval syndrome: a Rosetta stone for sympathetic related ventricular tachyarrhythmias. Circulation 1991;84:1414–1419.
76 Wang Q, Shen J, Splawski I, et al. *SCN5A* mutations associated with an inherited cardiac arrhythmia, long QT syndrome. Cell 1995;80:805–811.
77 Mohler PJ, Schott JJ, Gramolini AO, et al. Ankyrin-B mutation causes type 4 long-QT cardiac arrhythmia and sudden cardiac death. Nature 2003;421:634–639.
78 Plaster NM, Tawil R, Tristani-Firouzi M, et al. Mutations in Kir2.1 cause the developmental and episodic electrical phenotypes of Andersen's syndrome. Cell 2001;105:511–519.
79 Curran ME, Splawski I, Timothy KW, Vincent GM, Green ED, Keating MT. A molecular basis for cardiac arrhythmia: *HERG* mutations cause long QT syndrome. Cell 1995;80:795–803.
80 Wang Q, Curran ME, Splawski I, et al. Positional cloning of a novel potassium channel gene: *KVLQT1* mutations cause cardiac arrhythmias. Nat Genet 1996;12:17–23.
81 Splawski I, Tristani-Firouzi M, Lehmann MH, Sanguinetti MC, Keating MT. Mutations in the hminK gene cause long QT syndrome and suppress I_{Ks} function. Nat Genet 1997;17:338–340.
82 Vatta M, Ackerman MJ, Ye B, et al. Mutant caveolin-3 induces persistent late sodium current and Is associated with long-QT syndrome. Circulation 2006;114:2104–2112.

83 Domingo AM, Kaku T, Tester DJ, et al. AB16-6: sodium channel β4 subunit mutation causes congenital long QT syndrome [Abstract]. Heart Rhythm 2006;3:S34.

84 Bednar MM, Harrigan EP, Anziano RJ, Camm AJ, Ruskin JN. The QT interval. Prog Cardiovasc Dis 2001;43:1–45.

85 Tomaselli GF, Marban E. Electrophysiological remodeling in hypertrophy and heart failure. Cardiovasc Res 1999;42:270–283.

86 Sipido KR, Volders PG, De Groot SH, et al. Enhanced Ca(2+) release and Na/Ca exchange activity in hypertrophied canine ventricular myocytes: potential link between contractile adaptation and arrhythmogenesis. Circulation 2000;102:2137–2144.

87 Volders PG, Sipido KR, Vos MA, et al. Downregulation of delayed rectifier K(+) currents in dogs with chronic complete atrioventricular block and acquired torsades de pointes. Circulation 1999;100:2455–2461.

88 Undrovinas AI, Maltsev VA, Sabbah HN. Repolarization abnormalities in cardiomyocytes of dogs with chronic heart failure: role of sustained inward current. Cell Mol Life Sci 1999;55:494–505.

89 Maltsev VA, Sabbah HN, Higgins RS, Silverman N, Lesch M, Undrovinas AI. Novel, ultraslow inactivating sodium current in human ventricular cardiomyocytes. Circulation 1998;98:2545–2552.

90 Roden DM. Long QT syndrome: reduced repolarization reserve and the genetic link. J Intern Med 2006;259:59–69.

91 Belardinelli L, Antzelevitch C, Vos MA. Assessing predictors of drug-induced Torsade de Pointes. Trends Pharmacol Sci 2003;24:619–625.

92 Antzelevitch C, Shimizu W. Cellular mechanisms underlying the long QT syndrome. Curr Opin Cardiol 2002;17:43–51.

93 Shimizu W, Antzelevitch C. Effects of a K(+) channel opener to reduce transmural dispersion of repolarization and prevent Torsade de Pointes in LQT1, LQT2, and LQT3 models of the long-QT syndrome. Circulation 2000;102:706–712.

94 Shimizu W, Antzelevitch C. Differential effects of beta-adrenergic agonists and antagonists in LQT1, LQT2 and LQT3 models of the long QT syndrome. J Am Coll Cardiol 2000;35:778–786.

95 Ueda N, Zipes DP, Wu J. Prior ischemia enhances arrhythmogenicity in isolated canine ventricular wedge model of long QT 3. Cardiovasc Res 2004;63:69–76.

96 Ueda N, Zipes DP, Wu J. Functional and transmural modulation of M cell behavior in canine ventricular wall. Am J Physiol Heart Circ Physiol 2004;287:H2569–H2575.

97 Akar FG, Yan GX, Antzelevitch C, Rosenbaum DS. Unique topographical distribution of M cells underlies reentrant mechanism of torsade de pointes in the long-QT syndrome. Circulation 2002;105:1247–1253.

98 Emori T, Antzelevitch C. Cellular basis for complex T waves and arrhythmic activity following combined I(Kr) and I(Ks) block. J Cardiovasc Electrophysiol 2001;12:1369–1378.

99 Opthof T, Coronel R, Wilms-Schopman FJ, et al. Dispersion of repolarization in canine ventricle and the electrocardiographic T wave: T(p–e) interval does not reflect transmural dispersion. Heart Rhythm 2007;4:341–348.

100 Yuan S, Kongstad O, Hertervig E, Holm M, Grins E, Olsson B. Global repolarization sequence of the ventricular endocardium: monophasic action potential mapping in swine and humans. PACE 2001;24:1479–1488.

101 Yamaguchi M, Shimizu M, Ino H, et al. T wave peak-to-end interval and QT dispersion in acquired long QT syndrome: a new index for arrhythmogenicity. Clin Sci (Lond) 2003;105:671–676.

102 Castro HJ, Antzelevitch C, Tornes BF, et al. Tpeak-Tend and Tpeak-Tend dispersion as risk factors for ventricular tachycardia/ventricular fibrillation in patients with the Brugada syndrome. J Am Coll Cardiol 2006;47:1828–1834.

103 Wolk R, Stec S, Kulakowski P. Extrasystolic beats affect transmural electrical dispersion during programmed electrical stimulation. Eur J Clin Invest 2001;31:293–301.

104 Tanabe Y, Inagaki M, Kurita T, et al. Sympathetic stimulation produces a greater increase in both transmural and spatial dispersion of repolarization in LQT1 than LQT2 forms of congenital long QT syndrome. J Am Coll Cardiol 2001;37:911–919.

105 Frederiks J, Swenne CA, Kors JA, et al. Within-subject electrocardiographic differences at equal heart rates: role of the autonomic nervous system. Pflugers Arch 2001;441:717–724.

106 Shimizu M, Ino H, Okeie K, et al. T-peak to T-end interval may be a better predictor of high-risk patients with hypertrophic cardiomyopathy associated with a cardiac troponin I mutation than QT dispersion. Clin Cardiol 2002;25:335–339.

107 Takenaka K, Ai T, Shimizu W, et al. Exercise stress test amplifies genotype-phenotype correlation in the LQT1 and LQT2 forms of the long-QT syndrome. Circulation 2003;107:838–844.

108 Watanabe N, Kobayashi Y, Tanno K, et al. Transmural dispersion of repolarization and ventricular tachyarrhythmias. J Electrocardiol 2004;37:191–200.

109 Schwartz PJ, Priori SG, Spazzolini C, et al. Genotype-phenotype correlation in the long-QT syndrome: gene-specific triggers for life-threatening arrhythmias. Circulation 2001;103:89–95.

110 Antzelevitch C, Belardinelli L, Zygmunt AC, et al. Electrophysiologic effects of ranolazine: a novel anti-anginal agent with antiarrhythmic properties. Circulation 2004;110:904–910.

111 Antzelevitch C. Drug-induced channelopathies. In: Zipes DP, Jalife J, eds. *Cardiac Electrophysiology. From Cell to Bedside*, 4th ed. New York: WB Saunders; 2004:151–157.

112 Fenichel RR, Malik M, Antzelevitch C, et al. Drug-induced torsade de pointes and implications for drug development. J Cardiovasc Electrophysiol 2004;15:475–495.

113 Di Diego JM, Belardinelli L, Antzelevitch C. Cisapride-induced transmural dispersion of repolarization and torsade de pointes in the canine left ventricular wedge preparation during epicardial stimulation. Circulation 2003;108:1027–1033.

114 Sicouri S, Moro S, Litovsky SH, Elizari MV, Antzelevitch C. Chronic amiodarone reduces transmural dispersion of repolarization in the canine heart. J Cardiovasc Electrophysiol 1997;8:1269–1279.

115 van Opstal JM, Schoenmakers M, Verduyn SC, et al. Chronic Amiodarone evokes no Torsade de Pointes arrhythmias despite QT lengthening in an animal model of acquired long-QT syndrome. Circulation 2001;104:2722–2727.

116 Gussak I, Brugada P, Brugada J, et al. Idiopathic short QT interval: a new clinical syndrome? Cardiology 2000;94:99–102.

117 Gussak I, Brugada P, Brugada J, Antzelevitch C, Osbakken M, Bjerregaard P. ECG phenomenon of idiopathic and paradoxical short QT intervals. Cardiac Electrophysiol Rev 2002;6:49–53.

118 Gaita F, Giustetto C, Bianchi F, et al. Short QT syndrome: a familial cause of sudden death. Circulation 2003;108:965–970.

119 Brugada R, Hong K, Dumaine R, et al. Sudden death associated with short QT-syndrome linked to mutations in HERG. Circulation 2003;109:30–35 .

120 Bellocq C, Van Ginneken AC, Bezzina CR, et al. Mutation in the KCNQ1 gene leading to the short QT-interval syndrome. Circulation 2004;109:2394–2397.

121 Extramiana F, Antzelevitch C. Amplified transmural dispersion of repolarization as the basis for arrhythmogenesis in a canine ventricular-wedge model of short-QT syndrome. Circulation 2004;110:3661–3666.

122 Akar FG, Rosenbaum DS. Transmural electrophysiological heterogeneities underlying arrhythmogenesis in heart failure. Circ Res 2003;93:638–645.

123 Akar FG, Tomaselli GF. Conduction abnormalities in nonischemic dilated cardiomyopathy: basic mechanisms and arrhythmic consequences. Trends Cardiovasc Med 2005;15:259–264.

124 Vos MA, Jungschleger JG. Transmural repolarization gradients in vivo: the flukes and falls of the endocardium. Cardiovasc Res 2001;50:423–425.

125 van Opstal JM, Verduyn SC, Leunissen HD, De Groot SH, Wellens HJ, Vos MA. Electrophysiological parameters indicative of sudden cardiac death in the dog with chronic complete AV-block. Cardiovasc Res 2001;50: 354–361.

126 Yan GX, Joshi A, Guo D, et al. Phase 2 reentry as a trigger to initiate ventricular fibrillation during early acute myocardial ischemia. Circulation 2004;110:1036–1041.

127 Di Diego JM, Antzelevitch C. Cellular basis for ST-segment changes observed during ischemia. J Electrocardiol 2003;36(Suppl):1–5.

128 Antzelevitch C. The Brugada syndrome: diagnostic criteria and cellular mechanisms. Eur Heart J 2001;22:356–363.

129 Antzelevitch C, Oliva A. Amplification of spatial dispersion of repolarization underlies sudden cardiac death associated with catecholaminergic polymorphic VT, long QT, short QT and Brugada syndromes. J Intern Med 2006;259:48–58.